Catalysis Today 140 (2009) 187–191

Contents lists available at ScienceDirect

Catalysis Today

journal homepage: www.elsevier.com/locate/cattod

Hydrodesulphurization performance of NiW/TiO_2-Al_2O_3 catalyst for ultra clean diesel

Aijun Duan [a], Ruili Li [a], Guiyuan Jiang [a], Jinsen Gao [a,*], Zhen Zhao [a,*], Guofu Wan [a], Dengqian Zhang [a], Weiqiang Huang [a], Keng H. Chung [b]

[a] State Key Laboratory of Heavy Oil Processing, Faculty of Chemical Science and Engineering, China University of Petroleum, Xuefu Road 18#, Beijing 102249, PR China
[b] Well Resources Inc., 3919-149A Street, Edmonton, Alberta T6R 1J8, Canada

ARTICLE INFO

Article history:
Available online 5 December 2008

Keywords:
TiO_2-Al_2O_3 binary oxides
Sol–gel method
Hydrodesulphurization
NiW catalysts
Ultra clean diesel

ABSTRACT

TiO_2-Al_2O_3 binary oxide supports were obtained by sol–gel methods from Tetra-*n*-butyl-titanate and pseudoboehmite/aluminium chloride resources. The typical physico-chemical properties of NiW/TiO_2-Al_2O_3 catalysts with different TiO_2 loadings and their supports were characterized by means of BET, XRD and UV–vis DRS, etc. The BET results indicated that the specific surface areas of NiW/TiO_2-Al_2O_3 catalysts were as higher as that over pure γ-Al_2O_3 support, and the pore diameters were also large. The XRD and UV–vis DRS analyzing results showed that the Ti-containing supported catalysts existed as anatase TiO_2 species and the incorporation of TiO_2 could adjust the interaction between support and active metal, and impelled the higher reducibility of tungsten. The hydrodesulphurization (HDS) performance of the series catalysts were evaluated with diesel feedstock in a micro-reactor unit, and the HDS results showed that NiW/TiO_2-Al_2O_3 catalysts exhibited higher activities of ultra deep hydrodesulphurization of diesel oil than that of NiW/Al_2O_3 catalyst. The optimal TiO_2 content of NiW/TiO_2-Al_2O_3 catalysts was about 15 m%, and the corresponding HDS efficiency could reach to 100%. The sulphur contents of diesel products over NiW/TiO_2-Al_2O_3 (from pseudoboehmite/$AlCl_3$) catalysts with suitable TiO_2 content could be less than 15 ppmw, which met the sulphur regulation of Euro IV specification of ultra clean diesel fuel.

1. Introduction

Serious concern of stringent sulphur regulations and fuel specifications in many countries has imported the responsibility of pollution control to the refiners. The sulphur content of highway diesel fuel was required to reduce from a higher limit of 50 ppmw (in 2004) to a lower limit of 15 ppmw by 2006 in USA. This fuel, referred to as the ultra low sulphur diesel (ULSD), was legislated by the EPA to meet the 2007–2010 emission standards for heavy-duty engines, as well as the Tier 2 light-duty standards. In Europe the sulphur content of diesel is also expected to be lowered to 5–10 ppmw level after 2008 [1].

To realize this goal, one of the reasonable approaches is hydrotreating technology. The key points are the improvements and designs of active hydrodesulphurization (HDS) catalysts with better activity involving new phases of active metals and/or new types of materials [2–7]. The researchers paid more attentions to the development of new supports for hydrotreatment catalysts [8–10].

The composite supports including binary oxides of SiO_2, TiO_2, ZrO_2 modified γ-Al_2O_3 showed promising properties in catalysis processes [11–19]. The favorable reducibility and sulphurability of TiO_2-Al_2O_3 binary oxides made them facilitate to the redox processes of the active phases (Mo) [20–22], and help to form the active sites of octahedral Mo oxide species; therefore, it is expected to obtain a good HDS activity [23–25].

Yoshinaka and Segawa [26–29] prepared a series of TiO_2-Al_2O_3 composite supports by chemical vapor deposition (CVD) using $TiCl_4$ as a precursor. And they studied the conversion of Mo from oxidic to sulphdic state through sulphurization by X-ray photo-electron spectroscopy (XPS), which unambiguously revealed that the higher reducibility from oxidic to sulphidic molybdenum species on the TiO_2 and TiO_2-Al_2O_3 supports compared to that on the Al_2O_3 support. Higher TiO_2 loadings of the TiO_2-Al_2O_3 composite support led to higher reducibility and better dispersion for molybdenum species than on titania, which led to an increase of the number of HDS active centers known to be coordinatively unsaturated sites. The catalytic behavior over the TiO_2-Al_2O_3

* Corresponding author. Tel.: +86 10 89731586(O); fax: +86 10 69724721.
E-mail addresses: duanaijun@cup.edu.cn (A. Duan), jsgao@cup.edu.cn (J. Gao), zhenzhao@cup.edu.cn (Z. Zhao).

0920-5861/$ – see front matter © 2008 Elsevier B.V. All rights reserved.
doi:10.1016/j.cattod.2008.10.008

supported Mo catalysts, in particular for the 4,6-dimethyl-DBT, was much higher than that obtained over Al_2O_3 supported Mo catalyst. The ratio of the corresponding cyclohexylbenzene (CHB)/biphenyl (BP) derivatives were increased over the Mo/TiO_2-Al_2O_3. This indicated that the prehydrogenation of an aromatic ring played an important role on the HDS of DBT derivatives over TiO_2-Al_2O_3 supported catalysts [26]. The industrial HDS tests of straight run distillate gas oil showed that sulphide catalysts supported on TiO_2-Al_2O_3 composite (11 m%) could reduce the sulphur level of diesel fuel from 500 to 50 ppm under conventional hydrodesulphurization conditions [27]. HDS activities over NiMo/TiO_2-Al_2O_3 catalysts were more active than NiMo/Al_2O_3 catalysts for the model compound HDS of DBT, 4-MDBT and 4,6-DMDBT [28,29]. Ramirez and his cooperators [25,30] studied the detailed characterization of hydrotreating catalysts supported on TiO_2-Al_2O_3 binary oxides. They employed several methods to prepare TiO_2-Al_2O_3 binary oxides, involving mixing boehmite with the required amount of a solution of titanium isopropoxide in isopropanol. The suitable textural properties of the obtained TiO_2-Al_2O_3 binary oxides made the HDS efficiencies of NiMo/TiO_2-Al_2O_3 to be higher than that of NiMo/Al_2O_3 with Maya heavy crude feedstock [31].

The objective of this study was to prepare TiO_2-Al_2O_3 binary oxides using different alumina resources, and to investigate the influences of TiO_2 loadings of the NiW/TiO_2-Al_2O_3 catalysts on the HDS efficiency. In order to elucidate the suitable amount of TiO_2 incorporating to Al_2O_3, a series of TiO_2-Al_2O_3 supports were composed by sol–gel methods from the resources of Tetra-*n*-butyl-titanate and pseudoboehmite/aluminium chloride, and their relative NiW/TiO_2-Al_2O_3 catalysts with different TiO_2 contents of 5–30 m% were prepared and evaluated in the HDS of diesel feedstock. The prepared catalysts were characterized by N_2 physisorption, X-ray powder diffraction (XRD) and UV–vis diffuse reflectance spectra (DRS).

2. Experimental

2.1. Feedstocks

The feedstock was a blend of two commercial available diesels with the sulphur content of 432.49 μg g^{-1} concocted by Shengli FCC diesel and Fushun hydrotreating diesel. The properties of the diesel feedstock are shown in Table 1.

2.2. Catalyst preparation

2.2.1. Synthesis of TiO_2-Al_2O_3 binary oxides

A series of TiO_2-Al_2O_3 binary oxide supports were prepared by sol–gel method. The procedure follows the previous method of our group [11]. The titanium was derived from Tetra-*n*-butyl-titanate and the alumina was from pseudoboehmite or aluminium chloride.

Table 1
The typical properties of diesel feedstock.

Properties	Data
Density @ 20 °C/g cm^{-3}	0.8387
Sulphur/μg g^{-1}	432.49
Distillation/°C	
IBP	162
10%	224
30%	265
50%	298
70%	324
95%	369
FBP	453

The titanium sol was made from the Tetra-*n*-butyl-titanate, ethanol, nitric acid and deionized distilled water with the weight ratios shown in Table 2. Then the pseudoboehmite or aluminium was dissolved with certain proportional ethanol and nitric acid at certain temperature under the gently stirring condition for hours until aluminum-sol (Solution A) generated. Then titanium-sol was dripped into Solution A under drastic stirring condition. Afterwards, a gel formed and was dried in air for 10 h at 380 K and calcined at 773 K for 6 h. The composite supports were denoted as TiO_2-Al_2O_3-χ, where χ represented the TiO_2 content in composites.

2.2.2. Preparation of NiW/TiO_2-Al_2O_3 series catalysts

A series of NiW/TiO_2-Al_2O_3 catalysts were prepared by an incipient wetness impregnation method with an aqueous solution of the appropriate amounts of ammonium metatungstate hydrate $[(NH_4)_6W_{12}O_{39}{\cdot}H_2O]$ and nickel nitrate hexahydrate $[Ni(NO_3)_2{\cdot}6H_2O]$. The loadings of NiO and WO_3 active metal were 3.5 and 28 m%, respectively. After impregnation, the catalyst precursors were dispersed in an ultra-sonic unit for 30 min. Then the prepared samples were dried at 383 K for 12 h and calcined at 823 K for 5 h.

2.3. Characterization methods

2.3.1. Surface area, pore volume and pore size measurement

The typical physico-chemical properties of supports and catalysts were analyzed by BET method using Micromeritics adsorption equipment of ASAP 2000 (manufactured by Micromeritics Instruments Inc. USA). All the samples were outgassed at 673 K until the vacuum pressure was 6 μmHg. The adsorption isotherms for nitrogen were measured at 77 K. The surface area was calculated using the BET method based on adsorption data. The pore-size distribution for mesopore was analyzed from desorption branch of the isotherm by the Barrett–Joyner–Halenda (BJH) method and the pore-size distribution for micropore was analyzed by HK method.

2.3.2. X-ray diffraction analysis

XRD analyse of the samples were carried out on a XRD-6000 X-ray diffractometer using Cu Kα radiation under the setting conditions of 40 kV, 30 mA, scan range from 20 to 80° at a rate of 4° min^{-1}.

2.3.3. UV–vis diffuse reflectance spectroscopy

UV–vis diffuse reflectance spectra (DRS) experiments were performed on Hitachi U-4100 UV–vis spectrophotometer with the integration sphere diffuse reflectance attachment. The powder samples were loaded in a transparent quartz cell and were measured in the region of 200–800 nm at room temperature. The standard support reflectance was used as the baseline for the relative catalyst measurement.

2.4. Catalytic activities

Catalytic hydrotreating performances of the series catalysts were conducted in a high-pressure fixed-bed reactor with 2 g of catalyst (grain size of 0.3–0.5 mm). Firstly, catalysts were presulphided for 4 h with a 2 m% CS_2-cyclohexane mixture under the conditions of 593 K, 4 MPa, 1.0 h^{-1} and 600 cm^3 cm^{-3}. After presulphurization process, the inlet feedstock was switched to diesel and the operation conditions were regulated to be 623 K, 5 MPa, 1.0 h^{-1} and 600 cm^3 cm^{-3}.

Catalytic activities of hydrodesulphurization were tested under the above conditions after 13 h on-stream. HDS efficiencies of the appointed catalysts were evaluated by comparing of the sulphur

Table 2
Resources of support preparation from pseudoboehmite/$AlCl_3$.

$TiO_2/(TiO_2 + Al_2O_3)$/m%	$Ti(OC_4H_9)_4$/m%	C_2H_5OH/m%	H_2O/m%	HNO_3/m%	Pseudoboehmite or $AlCl_3$/m%
0	0.00	0.00	0.00	0.00	4.74
5	0.21	0.43	0.03	0.01	4.50
8	0.34	0.69	0.05	0.02	4.36
12	0.51	1.04	0.08	0.03	4.17
16	0.68	1.38	0.11	0.04	3.98
20	0.85	1.73	0.14	0.05	3.79
24	1.02	2.08	0.16	0.06	3.60
30	1.28	2.60	0.20	0.07	3.32
50	2.13	4.32	0.34	0.12	2.37
100	4.26	8.65	0.68	0.24	0.00

contents in product and diesel feed. The analysis methods of sulphur were described in our previous paper [11].

3. Results and discussion

3.1. Typical physico-chemical properties of TiO_2-Al_2O_3 binary oxides

3.1.1. Specific surface area and pore volume of TiO_2-Al_2O_3 composites

The typical textural properties of TiO_2-Al_2O_3 binary oxide supports are presented in Table 3.

The data in Table 3 show that the specific surface areas of TiO_2-Al_2O_3 binary oxide supports decrease with increasing TiO_2 loadings, since TiO_2 was usually a substance with a lower surface area and pore volume. However, all of these surface areas still keep at high levels, which are favorable for providing a suitable site for the high and uniform dispersion of active components of nickel and tungsten. The volumes and average pore diameters of these TiO_2-Al_2O_3 supports are very similar during the TiO_2 loading range from 5 to 20 m%. This indicates that the lower TiO_2 loading doesn't affect the configurations of binary oxide composites. When the TiO_2 loading is 30 m%, the typical volume and pore diameter show an apparent decrease comparing with those composites with the lower TiO_2 loadings.

Fig. 1 presents the pore size distribution of TiO_2-Al_2O_3 supports (from pseudoboehmite). The pore distributions show that the most feasible pore sizes are between 4 and 15 nm, and some large pores exist at 20–100 nm. These wide-range distributions of pore sizes are propitious to the high dispersions of active metals and the diffusions of reactant molecules.

3.1.2. XRD analysis of TiO_2-Al_2O_3 composites

Figs. 2 and 3 show the XRD patterns of TiO_2-Al_2O_3 supports with different TiO_2 loadings from different alumina resources (pseudoboehmite or $AlCl_3$). The XRD patterns indicate that all of these Ti-containing binary oxide supports show the similar types of spectra, and the existed species on the composites are mostly anatase TiO_2 species at the high TiO_2 loadings. When the TiO_2 loadings are less than 10%, there is no typical TiO_2 signal and only the characteristic peaks of Al_2O_3 are present at 46° and 67°.

Table 3
The textural properties of TiO_2-Al_2O_3 composites (from pseudoboehmite).

Support	S_{BET} ($m^2\ g^{-1}$)	V_{BJH} ($cm^3\ g^{-1}$)	Average pore diameter/nm
γ-Al_2O_3	233.3	0.77	13.1
TiO_2-Al_2O_3-5	270.1	0.75	11.5
TiO_2-Al_2O_3-10	264.7	0.79	12.0
TiO_2-Al_2O_3-15	262.1	0.75	11.9
TiO_2-Al_2O_3-20	259.3	0.74	11.7
TiO_2-Al_2O_3-30	258.7	0.67	10.3
TiO_2	5.5	0.0053	3.91

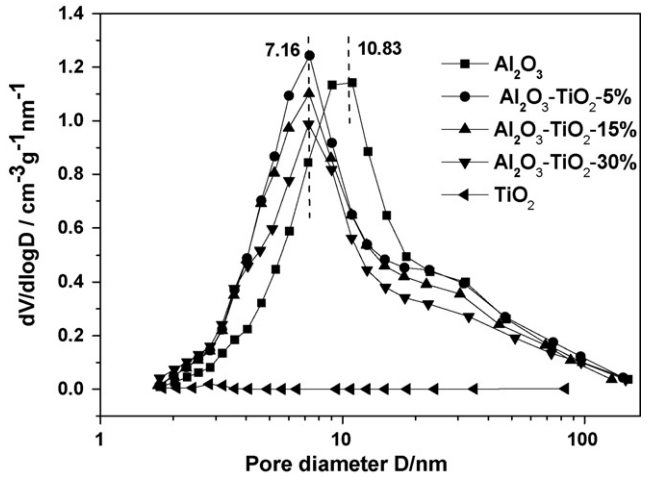

Fig. 1. Pore distribution of TiO_2-Al_2O_3 composite oxides (from pseudoboehmite).

3.2. Typical physico-chemical properties of NiW/TiO_2-Al_2O_3 catalysts

3.2.1. Specific surface area and pore volume of NiW/TiO_2-Al_2O_3 catalysts

Table 4 lists the typical physico-chemical properties of NiW/TiO_2-Al_2O_3 catalysts.

From data in Table 4, it can be seen that the specific surface areas of the catalysts decreased with the loading increases in TiO_2 content due to the low surface area and pore volume of TiO_2. Compared with the commercial Al_2O_3 support, the BET surface

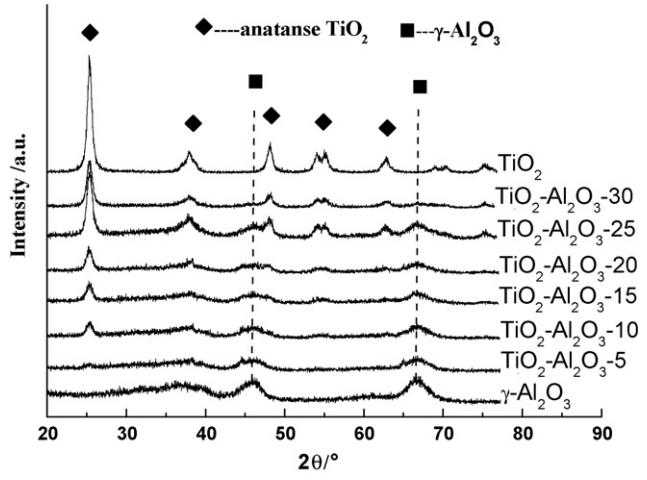

Fig. 2. XRD patterns of TiO_2-Al_2O_3 composite oxides (from pseudoboehmite).

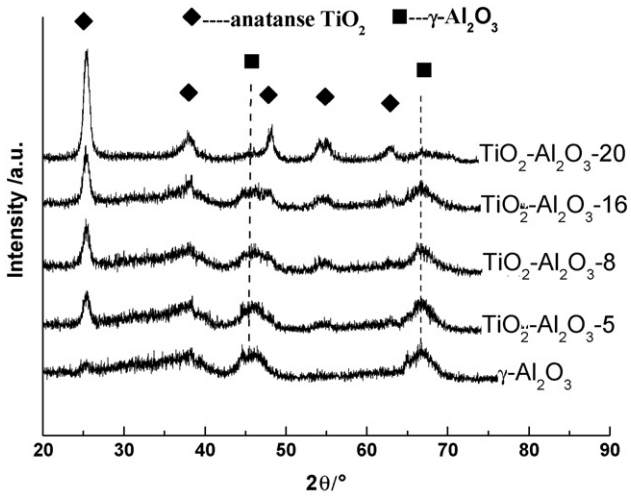

Fig. 3. XRD patterns of TiO_2-Al_2O_3 composite oxides (from $AlCl_3$).

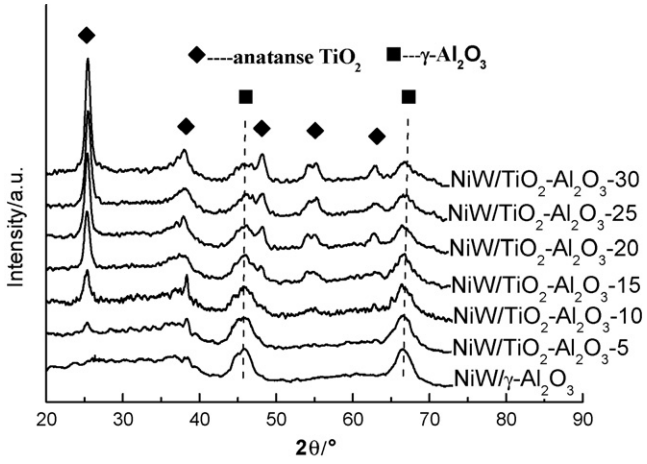

Fig. 4. XRD patterns of the NiW/TiO_2-Al_2O_3 catalysts (from pseudoboehmite).

areas of the Ti-incorporated catalyst samples were at a equivalent level and showed a slight downtrend with the further increasing of TiO_2 loadings. The high surface area facilitates to the high dispersion of nickel and tungsten active components, consequently, promotes the increase of HDS activity. The pore volumes of the catalysts decreased with the increases of TiO_2 loadings, but still kept at a higher level than that of the catalyst over the pure Al_2O_3 support. This confirmed that the incorporation of TiO_2 with Al_2O_3 did not affect the configuration of Al_2O_3 frame. The evidences of the higher average pore sizes of catalysts also confirmed the promising influence of Ti modification, since the higher pore sizes and surface areas facilitated the adsorption of large molecules including the refractory components as alkyl-substituted DBTs in diesel oil.

3.2.2. XRD analysis of NiW/TiO_2-Al_2O_3 catalysts

Fig. 4 shows the XRD patterns of the NiW/TiO_2-Al_2O_3 catalysts with different TiO_2 contents. It can be seen that there is no typical peak of WO_3 existed, indicating that the metal active component of tungsten over the catalyst surfaces are highly dispersed or the cluster of active phase is less than 3 nm. It is also known that Ti-containing supported catalysts exist mostly as anatase TiO_2 species. Because the anatase TiO_2 weakens the interactions between the active metal of tungsten and TiO_2-Al_2O_3 supports, the HDS activities of NiW/TiO_2-Al_2O_3 catalysts will be probably higher than that of Al_2O_3-supported catalyst [22–25].

3.2.3. UV–vis DRS analysis of NiW/TiO_2-Al_2O_3 catalysts

The UV–vis DRS was analyzed to determine the structures of the TiO_2-Al_2O_3 supported catalysts in the region from 200 to 800 nm as shown in Figs. 5 and 6. It can be observed that, compared with the one over the pure γ-Al_2O_3, the NiW/TiO_2-Al_2O_3 series catalysts showed broad absorption bands of ~250 and ~320 nm [32–34]. The intense adsorption band at about 260–340 nm is attributed to the ligand–metal charge transfer: $O^{2-} \rightarrow W^{6+}$ in W–O–W bridge bonds in polymeric structures [16,32]. The band around 250–280 nm is assigned to tetrahedron or octahedron tungstenic species. The band around 280–340 nm is ascribed to tungstic oxide and octahedron tungstenic species which make it more easy for the formation of coordinatively unsaturated or sulphur vacancies and thus it favor hydrodesulphurization reaction [33,34]. From Figs. 5 and 6, comparing the peak intensities around 300 nm, which were attributed to the octahedron tungstenic species, NiW/TiO_2-Al_2O_3 catalysts from pseudoboehmite (as shown in Fig. 5) show higher relative intensities than NiW/TiO_2-Al_2O_3 catalysts from $AlCl_3$ (as shown in Fig. 6). The differences between the peak intensities implied that the NiW/TiO_2-Al_2O_3 catalysts from pseudoboehmite resource formed more octahedron tungstenic species than NiW/TiO_2-Al_2O_3 catalysts from $AlCl_3$. That is the reason why the former catalysts (from pseudoboehmite) were more active than the latter. And this assumption could be confirmed by the following HDS results.

Table 4
The textural properties of NiW/TiO_2-Al_2O_3 catalysts (from pseudoboehmite).

Catalysts	S_{BET}/m^2 g^{-1}	V_{BJH}/cm^3 g^{-1}	Average pore diameter/nm
NiW/Al_2O_3	222.4	0.54	9.0
NiW/TiO_2-Al_2O_3-5	218.8	0.59	9.5
NiW/TiO_2-Al_2O_3-15	215.3	0.55	9.9
NiW/TiO_2-Al_2O_3-20	210.2	0.54	9.8
NiW/TiO_2-Al_2O_3-30	205.4	0.53	9.2

3.3. Catalytic HDS performances of NiW/TiO_2-Al_2O_3 catalysts

Tables 5 and 6 list the sulphur contents and HDS efficiencies of diesel products over NiW/TiO_2-Al_2O_3 series catalysts. The HDS efficiencies of NiW/TiO_2-Al_2O_3 (from $AlCl_3$) series catalysts in Table 4 exhibit very similar HDS efficiencies with different Ti contents, and the sulphur contents in products reach a minimum

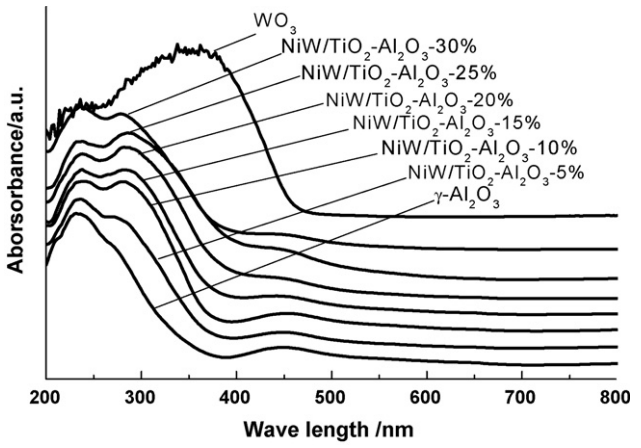

Fig. 5. UV–vis DR spectra of NiW/TiO_2-Al_2O_3 catalysts (from pseudoboehmite).

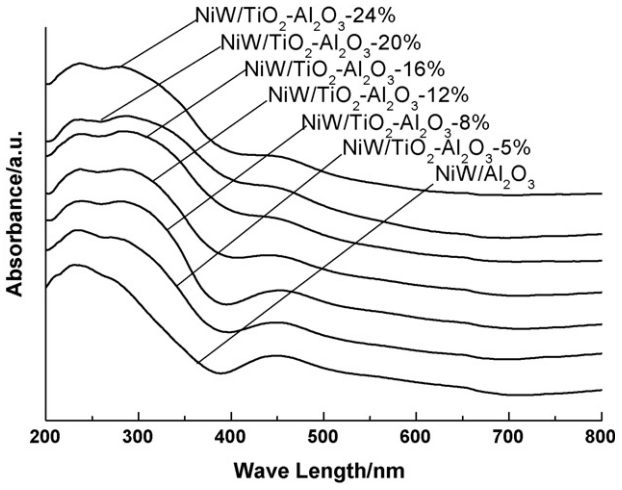

Fig. 6. UV–vis DR spectra of NiW/TiO_2-Al_2O_3 catalysts (from $AlCl_3$).

Table 5
HDS activities of NiW/TiO_2-Al_2O_3 (from $AlCl_3$) series catalysts.

Catalyst	TiO_2/m%	S/μg g^{-1}	HDS/%
Feed	–	432.49	–
NiW/γ-Al_2O_3	0	10.76	97.50
NiW/TiO_2-Al_2O_3-5	5	10.7	97.52
NiW/TiO_2-Al_2O_3-8	8	8.36	98.07
NiW/TiO_2-Al_2O_3-16	16	8.30	98.08
NiW/TiO_2-Al_2O_3-20	20	12.41	97.13

Table 6
HDS activities of NiW/TiO_2-Al_2O_3 (from pseudoboehmite) series catalysts.

Catalyst	TiO_2/m%	S/μg g^{-1}	HDS/%
NiW/γ-Al_2O_3	0	12.72	97.10
NiW/TiO_2-Al_2O_3-5	5	<0.02	~100
NiW/TiO_2-Al_2O_3-15	15	<0.02	~100
NiW/TiO_2-Al_2O_3-20	20	5.63	98.66
NiW/TiO_2-Al_2O_3-25	25	20.86	95.04
NiW/TiO_2-Al_2O_3-30	30	20.87	95.03

value at $TiO_2/(TiO_2 + Al_2O_3)$ ratio around 16%, which is lower than that of NiW/γ-Al_2O_3 catalyst. Meanwhile, for the NiW/TiO_2-Al_2O_3 (from pseudoboehmite) series catalysts, with the increasing of TiO_2 loading, the HDS efficiencies reach a maximum value (~100%) at $TiO_2/(TiO_2 + Al_2O_3)$ ratio of 15%, which is consistent with our previous researches over $NiMo/TiO_2$-Al_2O_3 catalysts [11]. The favorable sulphur content of diesel product on $NiMo/TiO_2$-Al_2O_3-15 catalyst is close to zero, which accords with the required standard of ultra clean diesel. As for the HDS efficiencies, the HDS activities of NiW/TiO_2-Al_2O_3 series catalysts from pseudoboehmite resources are much better than that from $AlCl_3$ resources, since the surface areas of TiO_2-Al_2O_3 composites from $AlCl_3$ resources are lower than those from pseudoboehmite resources. This maybe due to the inorganic Cl^- influence on the precipitation TiO_2-Al_2O_3 composites, furthermore resulted in the minor difference of their configuration. However, when the TiO_2 contents is between 5 and 20 m%, all the NiW/TiO_2-Al_2O_3 (both from pseudoboehmite/$AlCl_3$) catalysts could produce the diesel products with the sulphur contents less than 15 ppmw, which can also meet the sulphur regulation of Euro IV specification of ultra clean diesel fuel. The outstanding HDS performances of NiW/TiO_2-Al_2O_3 (from pseudoboehmite/$AlCl_3$) catalysts could be attributed to the reason that the Ti incorporation into Al_2O_3 weakened the interaction between the active metal and support, and resulted in the higher reducibility of tungsten on Al_2O_3-TiO_2 support.

4. Conclusion

In this paper, TiO_2-Al_2O_3 supports prepared by sol–gel methods from Tetra-*n*-butyl-titanate and pseudoboehmite/aluminium chloride resources showed the high specific surfaces and suitable pore diameters. The physico-chemical properties of NiW/TiO_2-Al_2O_3 catalysts and their supports were characterized by XRD and UV–vis DRS techniques. The analyzing results showed that the Ti-containing supported catalysts existed as anatase TiO_2 species and the incorporation of TiO_2 could adjust the interaction between support and active metal, and impelled the higher reducibility of tungsten. HDS efficiencies of NiW/TiO_2-Al_2O_3 series catalysts possessed the higher activities of ultra deep hydrodesulphurization of diesel oil than that of NiW/Al_2O_3 catalysts. The optimal TiO_2 content was about 15 m%, and the best HDS efficiency could reach to 100%. The sulphur contents of diesel products over NiW/TiO_2-Al_2O_3 (from pseudoboehmite/$AlCl_3$) catalysts with suitable TiO_2 content could be less than 15 ppmw, and met the sulphur regulation of Euro IV specification of ultra clean diesel fuel.

Acknowledgment

The authors acknowledge the financial supports from National Basic Research Program of China (No. 2004CB217806), National Natural Science Foundation of China (no. 20876173 and 20525021), the CNPC Innovation Foundation (05E7019) and the SKLHOP Program (2004-06).

Reference

[1] T.C. Ho, Catal. Today 98 (2004) 3.
[2] E. Furimsky, Appl. Catal. A 204 (2003) 1.
[3] D. Solís, A.L. Agudo, J. Ramírez, T. Klimova, Catal. Today 116 (2006) 469.
[4] N. Kunisada, K. Choi, Y. Korai, I. Mochida, K. Nakano, Appl. Catal. A 276 (2004) 51.
[5] T. Klimova, D. Solís, J. Ramírez, A. López-Agudo, Stud. Surf. Sci. Catal. 143 (2002) 267.
[6] D. Solís, T. Klimova, R. Cuevas, J. Ramírez, A.L. Agudo, Catal. Today 98 (2004) 201.
[7] X. Ma, L. Sun, C. Song, Catal. Today 77 (2002) 107.
[8] G. Murali Dhar, B.N. Snirivas, M.S. Rana, Manoj Kumar, S.K. Maity, Catal. Today. 86 (2003) 45.
[9] C. Song, X. Ma, Appl. Catal. B 41 (2003) 207.
[10] U.T. Turaga, C.S. Song, MCM-41 supported Co–Mo catalysts for deep hydrodesulfurization of light cycle oil, Catal. Today 86 (2003) 129–140.
[11] A. Duan, G. Wan, Z. Zhao, C. Xu, Y. Zheng, Y. g Zhang, T. Dou, X. Bao, K. Chung, Catal. Today 119 (2007) 13.
[12] M.C. Barrera, M. Viniegra, J. Escobar, M. Vrinat, J.A. de los Reyes, F. Murrieta, J. García, Catal. Today 98 (2004) 131.
[13] Z.B. Wei, W.H. Yan, H. Zhang, et al. Appl. Catal. A 167 (1998) 39.
[14] S. Damyanova, L. Petrov, M.A. Centeno, P. Grange, Appl. Catal. A 224 (2002) 271.
[15] M.S. Rana, S.K. Maity, J. Ancheyta, G.M. Dhar, T.S.R.P. Rao, Appl. Catal. A 268 (2004) 89.
[16] M.J. Vissenberg, Y. van der Meer, E.J.M. Hensen, V.H.J. de Beer, A.M. van der Kraan, R.A. van Santen, J.A.R. van Veen, J. Catal. 198 (2001) 151.
[17] R.M. Serna, J. Porous Mater. 10 (2003) 31.
[18] J.M. Vivar, R.M. Serna, J.G. Lara, R. Gaviño, J. Sol–Gel Sci. Technol. 8 (1997) 235.
[19] J.M. Vivar, R.M. Serna, P. Bosch, V.H. Lara, J. Non-Cryst. Solids 248 (1999) 147.
[20] A.A. Cecílio, S.H. Pulcinell, C.V. Santilli, J. Sol–Gel Sci. Technol. 31 (2004) 87.
[21] J.R. Grzechowiak, J. Rynkowski, I. Wereszczako, Catal. Today 65 (2001) 225.
[22] S.K. Maity, J. Anheyta, M.S. Rana, P. Rayo, Energy Fuels 20 (2006) 427.
[23] M. Laniecki, M. Ignacik, Catal. Today 116 (2006) 400.
[24] J.R. Grzechowiak, I. Wereszczako-Zielińska, K. Mrozińska, Catal. Today 119 (2007) 23.
[25] J. Ramírez, L. Cedeño, G. Busca, J. Catal. 184 (1999) 59.
[26] S. Yoshinaka, K. Segawa, Catal. Today 45 (1998) 293.
[27] S. Yoshinaka, M. Nagata, T. Funamoto, et al. Appl. Catal. A 295 (2005) 11.
[28] K. Segawa, M. Katsuta, F. Kameda, Catal. Today 29 (1996) 215.
[29] S. Yoshinaka, K. Segawa, Catal. Today 86 (2003) 61.
[30] J. Ramírez, G. Macías, L. Cedeño, et al. Catal. Today 98 (2004) 19.
[31] J. Ramírez, P. Rayo, A.G. Alejandre, et al. Catal. Today 109 (2005) 54.
[32] A. Gutiérrez-Alejandre, J. Ramírez, G. Busca. Langmuir 14 (1998) 630.
[33] A. Gutiérrez-Alejandre, J. Ramírez, G. Busca, Catal. Lett. 56 (1998) 29.
[34] J. Ramírez, A. Gutiérrez-Alejandre, J. Catal. 170 (1999) 108.